Measurement of Internal Strain in Cast-concrete Structures

by William C. Stone

ABSTRACT—A practical method for experimentally measuring strain profiles inside cast-concrete structures is presented. The technique employs micro-embedment strain gages which are oriented along paths of interest inside the structural element prior to casting. Tests of numerous post-tensioned concrete-box-girder anchorage elements, and of large-scale pullout test specimens instrumented with micro-embedment gages have shown good agreement between the measured strains and those predicted by means of detailed finite-element analyses within the linear-elastic region of the material.

Introduction

A common practice in structural research work is to instrument a number of key experimental specimens for subsequent verification of an analytical model or solution technique. If the model accurately reproduces the measured behavior of the laboratory specimens, it can then be used for parametric studies at a significant savings of time and cost. In most cases, measurements of external deflections, surface strains, and reaction forces are all that are required to define the response of a structural system. Examples of such cases are the modeling of overall behavior of building frames and of bridge structures. For more complex three-dimensional structures, cast structural elements, and when trying to predict material failure, the above techniques are often insufficient for analysis. As examples, consider the task of experimentally determining the state of strain inside the anchorage zone of a post-tensioned concrete structure, along the critical internal-failure surface of an embedded tension anchor, or through the thickness of a concrete member under multiaxial states of loading. All of these are structural details in which the internal distributions of stress and strain are not uniquely indicated by the states of stress and strain at the surface.

William C. Stone is Research Structural Engineer, National Bureau of Standards, Washington, D.C. 20234.

Final manuscript received: July 11, 1983.

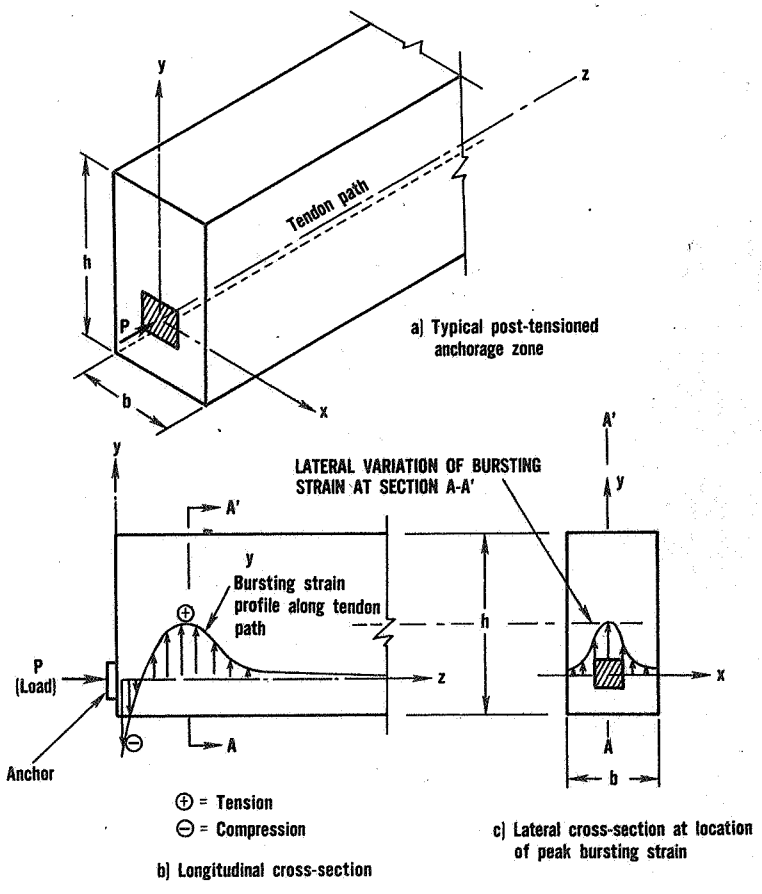

Fig. 1—Bursting-strain profiles along tendon path for a post-tensioned concrete-girder anchorage

From 1975 until 1981 the author was involved in experimental research with two of the above examples: a study of post-tensioned concrete-girder anchorage zones,[1] and a study of the pullout method of nondestructive strength evaluation of concrete.[2] Both of these studies sought to explain complex external performance characteristics by means of an analysis of the internal strain distribution. A brief description of the experimental specimens used in these two studies is given in the appendix.

To measure the internal strain distribution, in both cases it was necessary to have a reliable method by which the strain could be monitored without disrupting the strain field. It was also desired to have a sufficient number of measurements along the path of interest to completely define a particular strain profile. In the first case the 'bursting' strain ahead of the loaded anchor (Fig. 1) was to be measured. Laterally this strain is at a maximum along the center line of the post-tensioning tendon and decreases nonlinearly towards the side faces. In the second case the 'circumferential,' 'radial,' and 'axial' strain distributions (see Fig. 2 for the orientation convention) were to be measured along the idealized failure surface of a pullout test. In both situations the strain variation was to be monitored over a total distance of usually not more than 15 in. (38 cm). This meant that the measuring device would have to be very small and capable of detecting the strain in the concrete; i.e., it would require a positive embedment in the concrete in such a manner as to preclude the possibility of slippage. The available commercial embedment gages were much too large to be useful in such tests, so the gages used were fabricated in the laboratory.

Fabrication

A simple micro-embedment strain gage was developed as shown in Fig. 3. The embedment gage is composed of a foil strain gage bonded to an aluminum rod and represents a modified version of a similar embedment gage first developed by the author.[1] To meet the requirement of negligible slippage an enlarged anchor (f in Fig. 3) was attached to each end of the aluminum rod. The length of the rod between these two anchors was 1 in. (25.4 mm). Over this length the bond between the aluminum rod and the concrete was broken so that the foil gage measured the average strain in the concrete between the two end anchors. It should be noted that these gages measure only axial strain, parallel to the length of the rod. When linked to the laboratory data-acquisition system used for the above studies the accuracy of these gages was approximately ±6 microstrain.

An extensive search of available foil strain gages showed that the smallest workable 120-ohm gage had a gage length of 0.031 in. (0.78 mm) and a grid width of 0.032 in. (0.81 mm). A small gage was desirable for two reasons. First, a smaller gage allowed for the use of a smaller diameter rod. This minimized the interference caused by the embedment gage to the surrounding strain

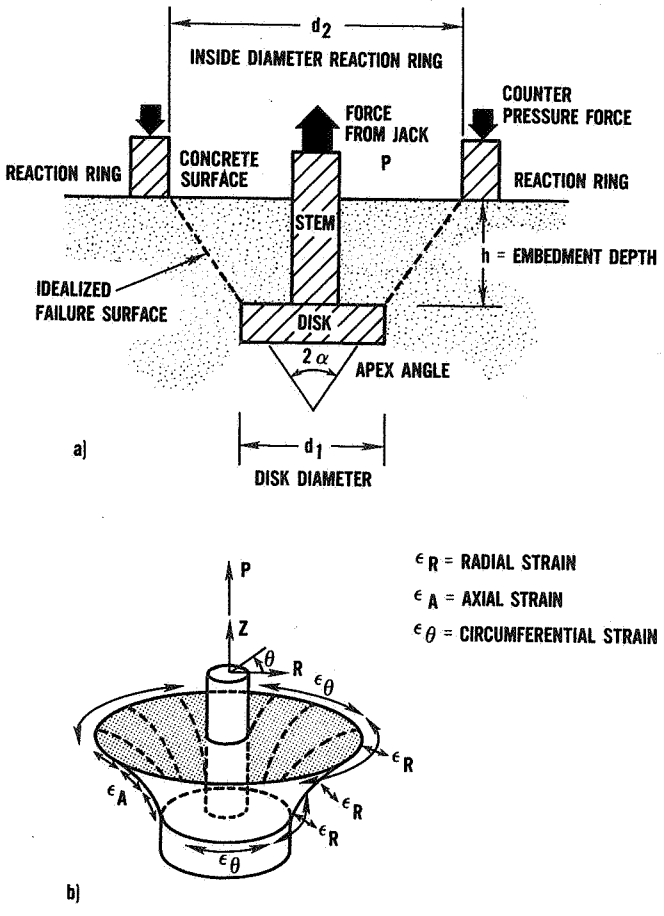

Fig. 2—Schematic representation of the pullout test in concrete

field. Secondly, since the gage is bonded to a round surface, a smaller strain gage meant less induced curvature to the gage during the bonding process.* To permit the strain gage to be bonded to a round surface, a flexible polyamide-backed variety was used. The foil gages were mounted on a 1.2-in. (32-mm) long, 0.135-in. (3.3-mm) diameter rod of 7075-T6 aluminum alloy which was pre-threaded for 1/8 in. (3.2 mm) on each end (see Fig. 3). Two gaging configurations are possible. (a) In locations where lateral bending of the rod is not expected to be a problem one foil gage located at the center of the rod will

A general rule of thumb is that the strain gage should occupy no more than a 45-degree segment around the circumference of the bar.

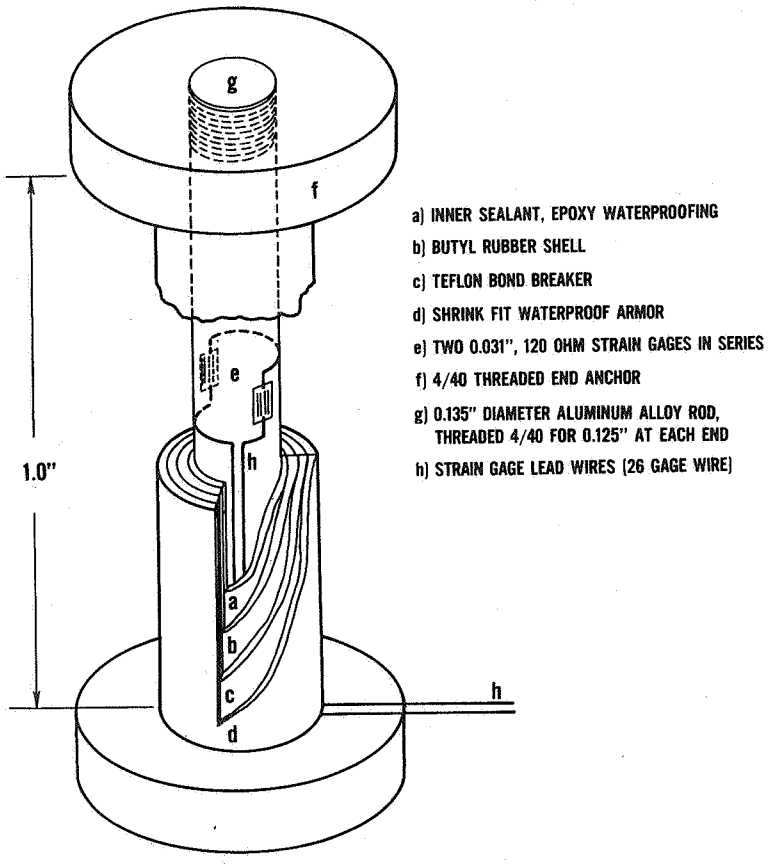

Fig. 3—Flexure-compensating-compliant micro-embedment concrete strain gage

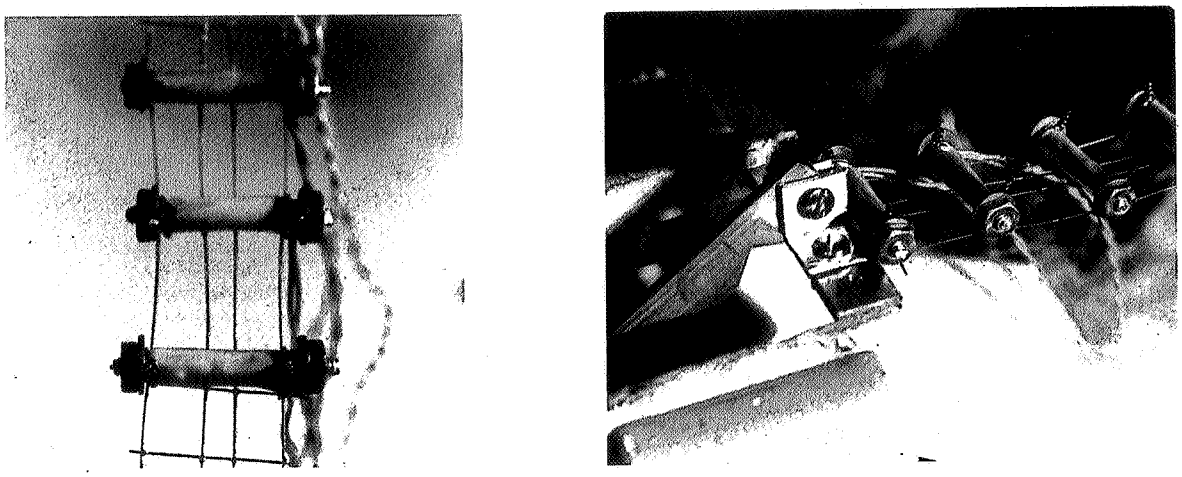

(a) (b)

Fig. 4—Typical gage-string details: (a) gages wired to piano-wire grid using flexible copper wire; (b) typical end detail for connection of gage string to pullout test specimen

give sufficiently accurate results so that a bending correction gage is not necessary. (b) Where the strain gradient across the end anchors is expected to be very large, such that the rod might experience large flexural deformations, a second foil gage mounted 180 degrees opposite the first foil gage (Fig. 3), and wired in series with it, will compensate for the bending effects.

For case (a) the data-acquisition bridge circuit has to be balanced with either an additional identical gage (for temperature compensation) or a precision 120-ohm resistor if the ambient temperature is relatively constant. For case (b) the bridge circuit has to be balanced with either an additional identical two-gage set (for temperature compensation) or a precision 240-ohm resistor if the ambient temperature is relatively constant.

A two-component methyl-cyanoacrylate adhesive was used for the bonding. The foil gages were waterproofed with a liquid epoxy sealant after the leadwires had been soldered in place (*a* in Fig. 3). The entire assembly was then encased in a thin shell of flexible butyl-rubber barrier compound (*b* in Fig. 3) and overwrapped with polytetrafluoroethylene tape (*c* in Fig. 3). An enlarged anchor (4-40 thread) measuring 3/8 in. (9 mm) in diameter and 0.125 in. (3 mm) thick was then attached on one end (where the leadwires exit) and the central portion of the gage was inserted into a 1-1/8-in. (28.5-mm) piece of ¼-in. (6.35-mm) diameter heat-shrink tubing which butted against the washer. A heat gun was used to shrink the tubing so that a durable waterproof shell encased the gage (*d* in Fig. 3). The anchor for the opposite end was

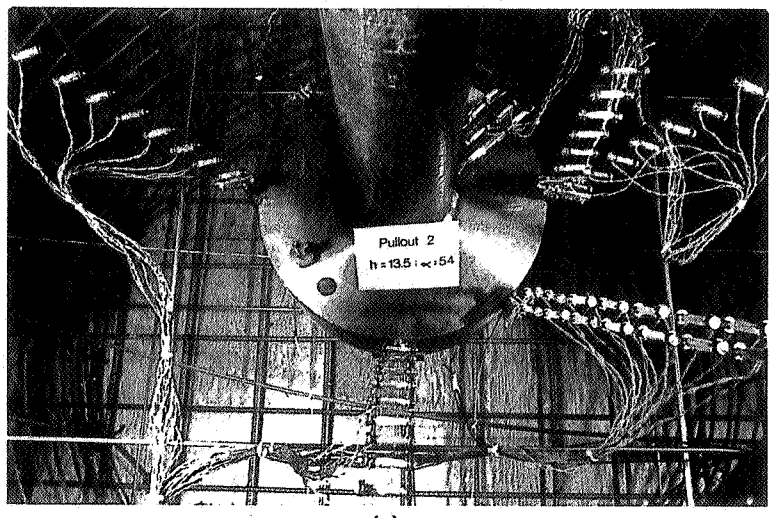

(a)

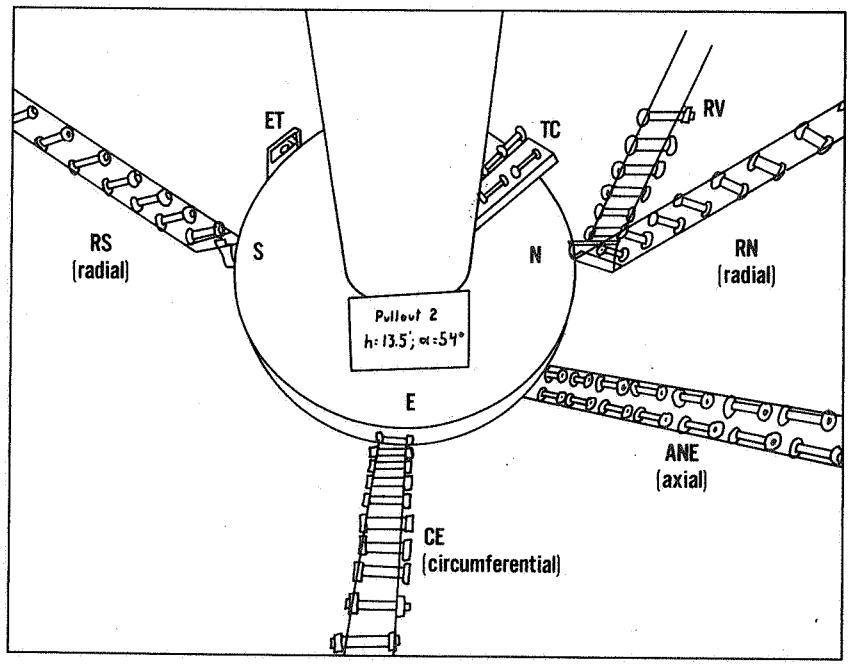

(b)

Fig. 5—Photo and isometric view of instrumented pullout specimen prior to concrete casting

then screwed on until snug and the embedment gage was tested to ensure proper electronic performance.

The butyl-rubber barrier compound and the protective outer shell described above also perform an extremely important function with regards to compliance between the gage and the surrounding concrete. By varying the thickness of the butyl layer the composite stiffness of the gage can be made to match that of the concrete. As an example the gages used in the investigation detailed in Ref. 2 were 0.25-in. (6.3-mm) in diameter when completed. The foil strain gages were mounted on a 0.135-in. (3.3-mm) diameter aluminum rod. For calculation of the composite stiffness the modulus of butyl rubber can be assumed to be negligible. The composite stiffness (modulus) is thus given by:

$$E_{composite} = \frac{E_{rod}A_{rod} + E_{butyl}A_{butyl}}{(A_{rod} + A_{butyl})} = \frac{10(10)^6\,(0.135)^2\,\pi/4 + 0}{(0.25)^2\,\pi/4}$$

$$= 2.92(10)^6 \text{ psi } (20.15 \text{ GPa}) \qquad (1)$$

This closely approximates the experimentally observed value for the modulus of the concrete, $E_c = 2.82(10)^6$ psi (19.5 GPa).

Placement

In order to measure a particular strain profile within the concrete under load it is necessary to have a string of closely spaced embedment gages suspended along the line of interest. This can be accomplished by attaching the gages with soft copper wires to a grid constructed from 0.016-in. (0.4-mm) stainless-steel piano wire, as shown in Fig. 4(a). In the pullout study each end of the grid was soldered to a brass bar, which was machined so that it could be bolted to attachment points on the disk edge of the pullout insert [Fig. 4(b)]. Typical gage strings, as placed prior to casting a large-scale pullout test specimen, are shown in Fig. 5.

To reduce the possibility of losing a strain measurement at a key location, redundant gage strings were employed. For the pullout study it was possible to place the redundant gage strings around the circumference of the pullout disk, owing to the symmetry of the test. Gage strings *RS* and *RN* shown in Fig. 5, for example, constituted a redundant set for measuring the radial strain (strain perpendicular to the failure surface). Alternatively, redundancy for axial strain measurement (strain parallel to the failure surface; see ANE gages, Fig. 5) was achieved by overlapping two parallel sets of gages. In most cases the gage loss rate during casting of concrete and testing was approximately 10 percent.

Performance

Figures 6, 7, 8 and 9 present typical results that have been obtained in various studies in which experimental

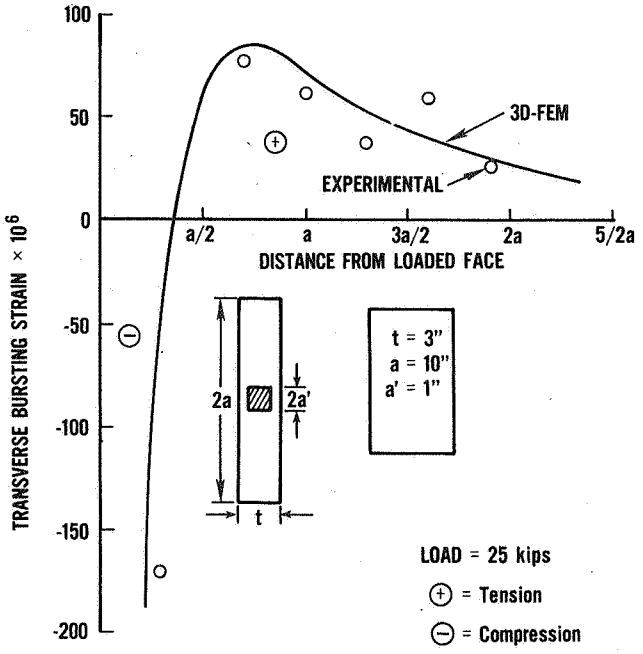

Fig. 6—Comparison of experimental and analytical transverse-bursting-strain distribution for a concentrically loaded post-tensioned anchorage (from Ref. 1)

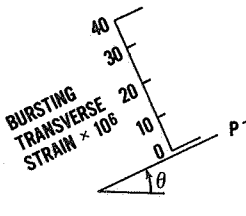

Fig. 7—Comparison of experimental and analytical transverse-bursting-strain distribution for a concentrically loaded post-tensioned anchorage with a 30-deg inclined tendon (from Ref. 1)

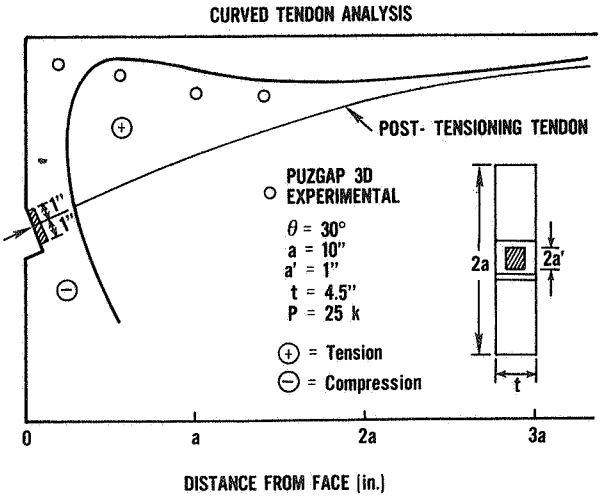

strains from the micro-embedment gages are compared with analytical findings from finite-element models (FEM). In Figs. 6 and 7, the experimentally measured transverse-bursting-strain distribution ahead of the loaded face of a post-tensioned bearing plate is compared with the results of a three-dimensional linear-elastic finite-element program.[3] At the indicated load (75 percent of maximum load) the specimen was still in an uncracked state. This allowed for a direct comparison with a linear-elastic FEM solution since the stress–strain relationship for concrete in tension is fairly linear, until loads sufficient to induce rupture.

As an example of the performance of the technique for measuring compressive strains, Figs. 8 and 9 show the axial (compressive) strain distribution along the idealized failure surface in a pullout test. The comparison was made with a linear-elastic-axisymmetric FEM analysis[2] at a load equal to 17 percent of the ultimate pullout load, which maintained concrete strains within the linear region of the stress–strain curve. Although the experimental scatter is somewhat higher here, the general trends and magnitudes of the measured strains are in good agreement with the finite-element solution. When one considers that concrete is not truly a homogeneous material, and that

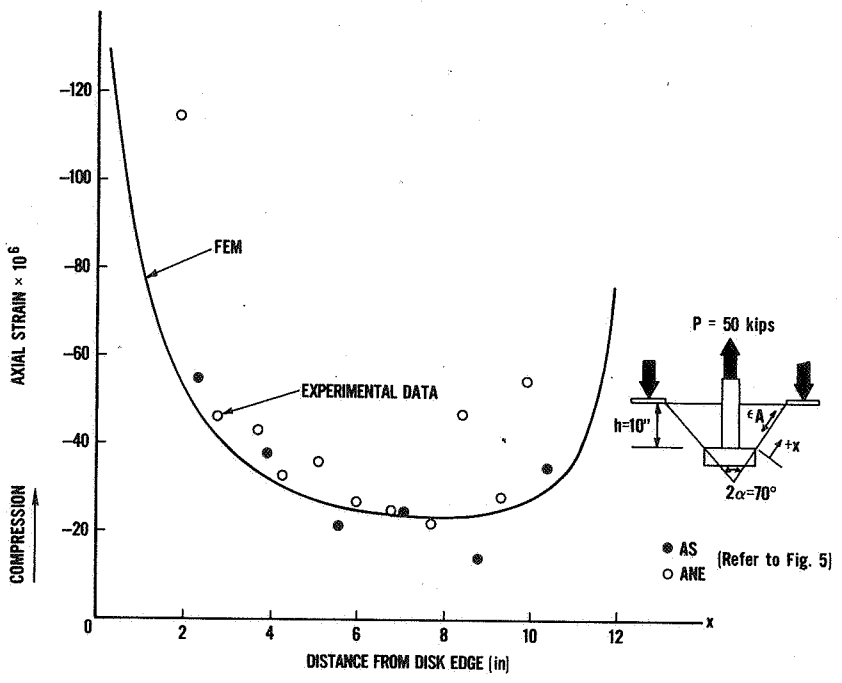

Fig. 8—Axial strain along idealized failure surface, experimental vs. finite-element solution. Specimen #1, apex angle = 70 deg (from Ref. 2)

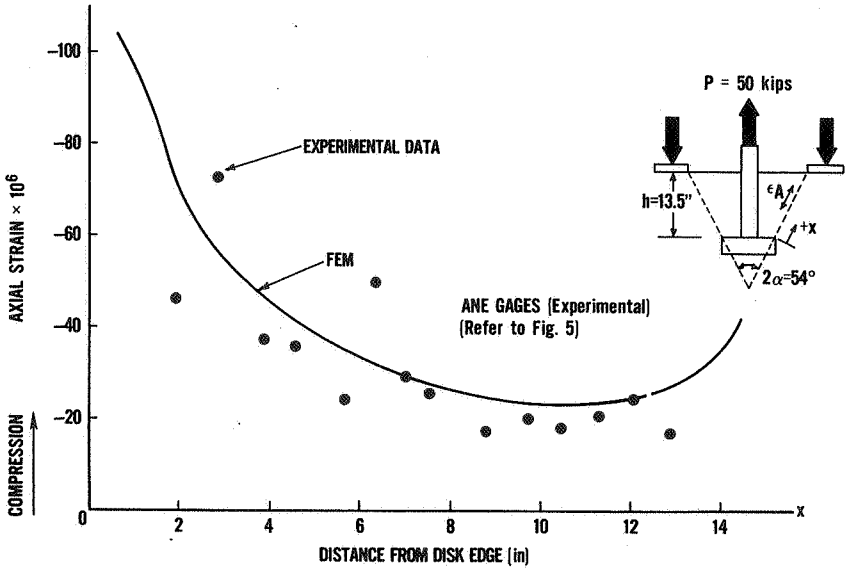

Fig. 9—Axial strain along idealized failure surface, experimental vs. finite-element solution. Specimen #2, apex angle = 54 deg (from Ref. 2)

localized changes in the stiffness and strain distribution are likely, these results are encouraging.

Although a single embedment gage will monitor only the internal strain parallel to the axis of the gage, it will not be necessary in most cases for the experimentalist to proceed to a more complex strain-measuring device for the sake of determining the internal state of stress. At this point one can directly compare the experimental strain data with the results of a finite-element analysis, which gives as standard output both the calculated states of strain and stress along any orientation (provided that the FEM mesh is consistent with the embedment-gage placement) throughout the entire structure. If agreement is found between the experimental and analytically calculated strains along all key profiles it can be assumed that the analytical model is correct and that the calculated state of stress is valid. Conversely, if there is no agreement it is evident that the mathematical model will require modification.

Conclusions

A practical method for experimentally measuring strain profiles inside cast-concrete structures is presented. The technique employs the use of micro-embedment strain gages which are oriented along paths of interest inside the structural element prior to casting. Tests of numerous post-tensioned concrete-girder anchorage elements and of large-scale pullout test specimens instrumented with micro-embedment gages have shown good agreement between the measured strains and those predicted by means of detailed finite-element analyses within the linear-elastic region of the material. A powerful tool is thus available for the analysis of complex cast shapes whereby a computational model can be verified by experimental determination of the internal state of strain.

References

1. *Stone, W.G., Paes-Filho, W. and Breen, J.E., "Behavior of Post-Tensioned Girder Anchorage Zones," Center for Transportation Research, #208-2, Austin, Texas (1981).*

2. *Stone, W.C., "Internal Strain, Deformation and Failure of Large Scale Pullout Tests in Concrete," NBS, Washington, D.C., NBSIR 82-2484 (1982).*

3. *Stone, W.C. and Breen, J.E., "Analyses of Post-Tensioned Girder Anchorage Zones," Center for Transportation Research, #208-1, Austin, Texas (1981).*

TABLE A1—MICROCONCRETE-MIX DESIGN FOR UNIVERSITY OF TEXAS TESTS

TCM 1/8 Aggregate	41.0 lb (18.6 Kg)
Ottawa Silica Sand	36.8 lb (16.7 Kg)
No. 1 Blast Sand	33.8 lb (15.4 Kg)
Type III Cement	21.25 lb (9.7 Kg)
Water	14.8 lb (6.7 Kg)
Water/Cement Ratio	0.7

TABLE A2—MIX DESIGN FOR NBS PULLOUT SPECIMENS

	Specimen #1	Specimen #2
Type I Cement (lbs)	3172 (1442 Kg)	2961 (1346 Kg)
Silicious Sand (lbs)	12015 (5461 Kg)	12816 (5825 Kg)
Pea Gravel (lbs)	11437 (5198 Kg)	12200 (5545 Kg)
Water (lbs)	2200 (1000 Kg)	2384 (1083 Kg)
W/C (approximate)	0.693	0.805

TABLE A3—CYLINDER-STRENGTH RESULTS NBS PULLOUT TESTS

	Compressive (psi)			Splitting Tension	
	Room Cure	CIPPOC	Slave	CIPPOC	Slave
Specimen #1 (age = 27 days)	2920 (89)*	2660 (86)	—	336 (15)	—
Specimen #2 (age = 13 days)	1345 (69)	1290 (44)	1180 (34)	174 (11)	129 (14)

**Standard deviation, psi*
1 psi = 0.0069 MPa

APPENDIX: Specimen Details from References 1 & 2

Figures A1 and A2 show the experimental specimens used in the post-tensioned anchorage-zone study at the University of Texas at Austin.[1,3] The prototype specimen (Fig. A1) was designed to replicate a typical web section of a post-tensioned segmental box-girder bridge. The prototype concrete for this study was based upon the Texas Department of Highways and Public Transportation Type H mix design for superstructure concrete, which is to say, a standard, Type I portland-cement based, ¾-in. (19-mm) maximum aggregate size concrete with a water-cement ratio of approximately 0.7 and a slump of 3 to 5 in. (7.6-12.7 cm). Compressive strength at the time of testing varied from 4500 to 6000 psi (31-41.4 MPa). The model specimens (Fig. A2) were precise ¼-scale replicates of the prototype. A special microconcrete was used for the model specimens. This was based on a geometric scaling of the prototype aggregate gradation curve with some modification of the scaled curve to reduce the water requirements created by the presence of very small particles. The final microconcrete mix used had the material quantities per cubic foot (0.0283 m^3) of mix as given in Table A1.

Microconcrete compressive strength at the time of testing varied from 3500 to 4600 psi (24.1-31.7 MPa). Embedment gages were placed along the tendon path (shown by the dashed line in Fig. A3) such that the orientation was parallel to the vertical side face of the specimen with the axis perpendicular to the tendon path. This was intended to monitor the bursting strain along the tendon path. The bursting tensile strain was of key interest in this study since previous failure theories for initiation of tendon-path cracking were based on bursting strains. Additional embedment gages placed along the loaded end face later indicated that end face 'spalling' tensile strains were the initiator of cracking in thin-web post-tensioned applications.[1,3]

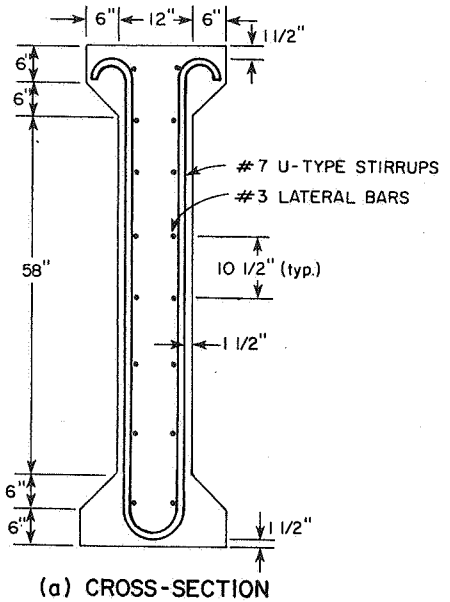

(a) CROSS-SECTION

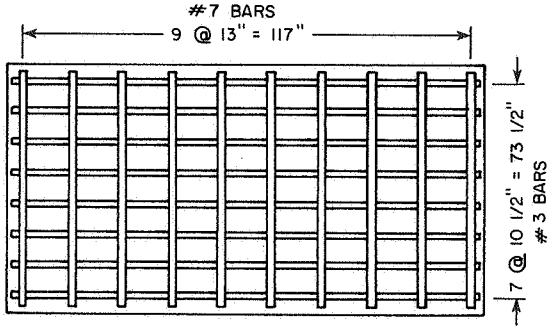

(b) ELEVATION

Fig. A1—Prototype box-girder web section used for the University of Texas anchorage-zone tests

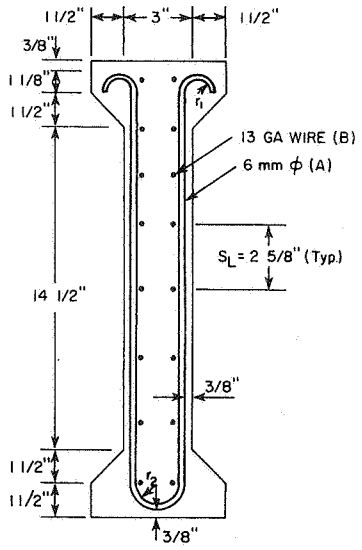

(a) CROSS-SECTION

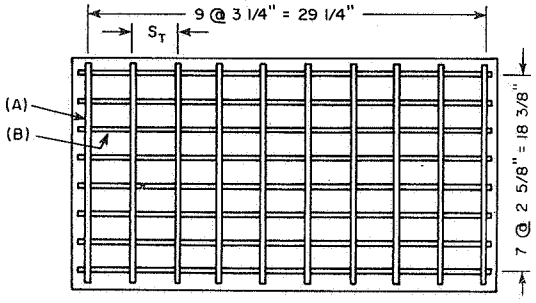

(b) ELEVATION

Fig. A2—One-quarter scale-model details used for the University of Texas anchorage-zone tests

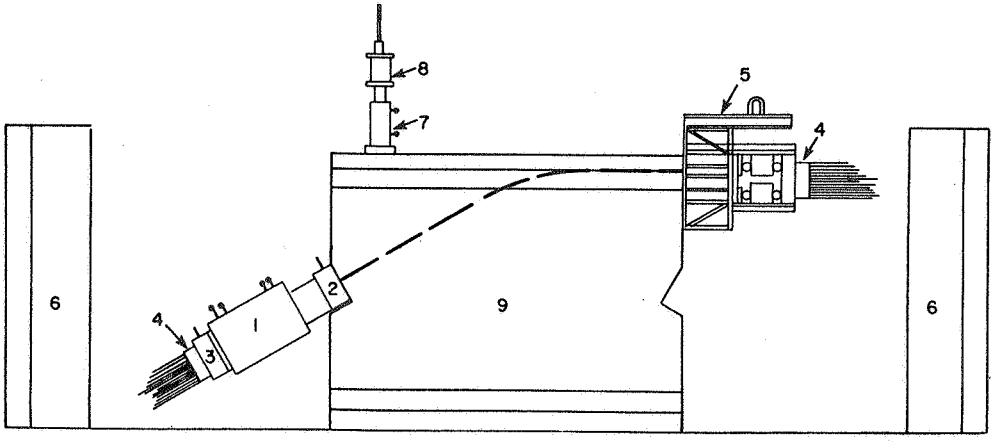

(1) 500 TON CENTER HOLE RAM
(2) SPACER BLOCK
(3) REAR SPACER BLOCK
(4) 26 STRAND ANCHOR HEAD
(5) DEAD MAN-FRICTION LOAD CELLS
(6) TENDON BACKSTOP
(7) LATERAL POST-TENSIONING JACK
(8) LOAD CELL FOR 7
(9) FULL SCALE CURVED TENDON SPECIMEN

Fig. A3—Overall view of prototype testbed for the University of Texas anchorage-zone tests

Figure A4 shows a typical specimen and the loading apparatus used during the first phase of the Bureau of Standards Pullout Test Project. The specimens represented a 12:1 scaled-up version of typically available commercial inserts. The increased scale permitted the placement of the large numbers of embedment gages necessary to define the internal strain profiles of interest. The critical area of interest in the pullout test is along the failure surface which forms approximately along the diagonal (shown in Fig. A4) from the outer disk edge (K) to the inside edge of the reaction ring (H). Embedment gages were placed as previously shown in Fig. 5. The mix designs used for the two specimens tested are given in Table A2.

Note that pea gravel was used for the 'coarse' aggregate portion of the mix. This was chosen because it was the smallest readily available commercial aggregate. The intent of this choice was to make the concrete mix as homogeneous as possible from the perspective of the scaled-up pullout insert. This would then allow for better correlation with the analytical model which assumed the concrete to behave as a perfectly homogeneous material. In-place strength of the concrete at the time of testing was determined by three methods: standard room-cured cylinders; cast-in-place push-out cylinders (CIPPOCS); and by slave cylinders cured in a temperature-controlled water bath. By means of a closed-loop thermocouple-driven system the slave cylinders were cured at the same temperature as the core of the specimen in the vicinity of the pullout insert. Results of these strength tests are given in Table A3.

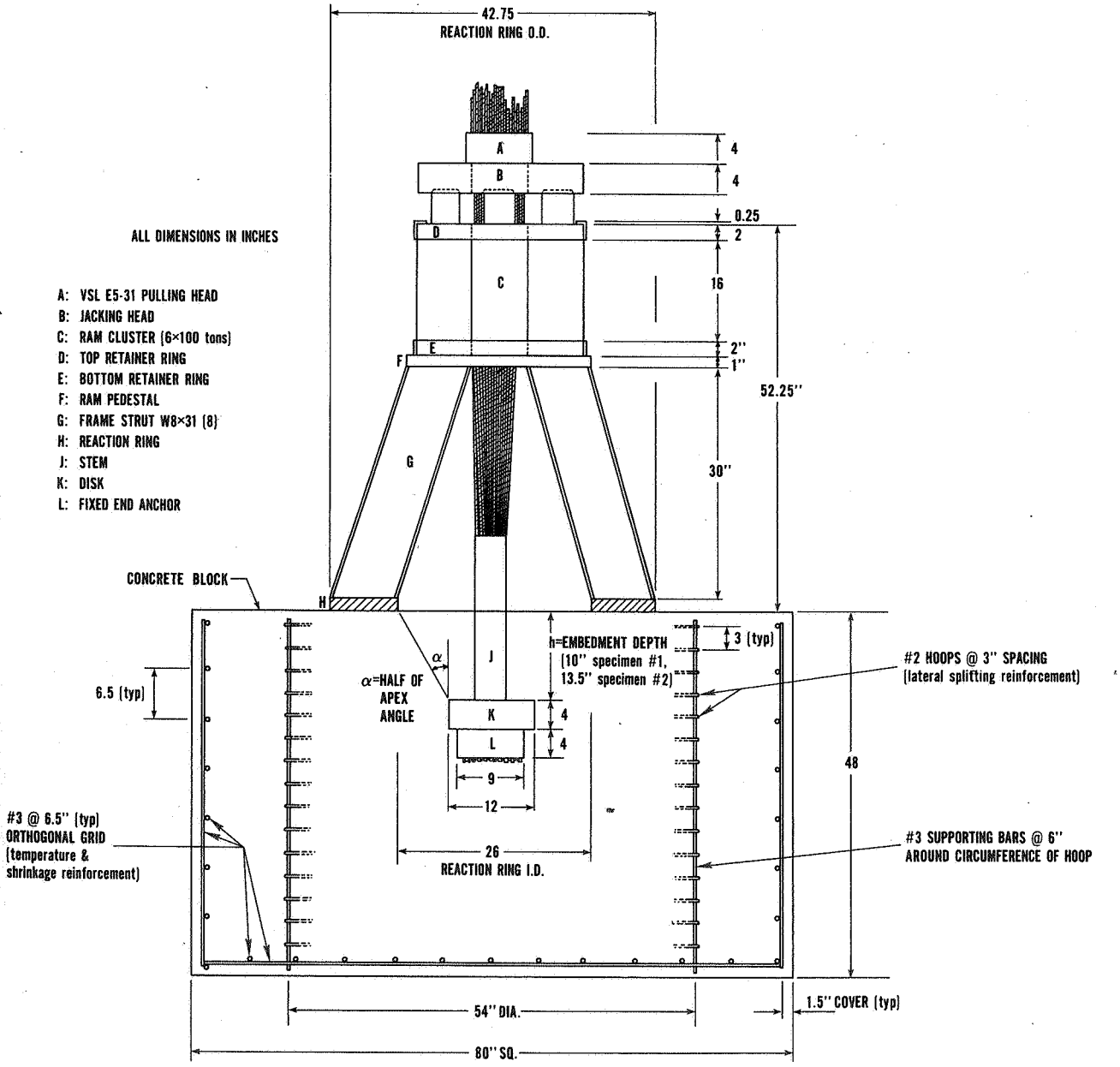

Fig. A4—Overall view of NBS large-scale pullout test